Nanoscale Research Letters
a SpringerOpen Journal

NANO EXPRESS Open Access

Scandium effect on the luminescence of Er-Sc silicates prepared from multi-nanolayer films

Adel Najar[1*], Hiroo Omi[1,2] and Takehiko Tawara[1,2]

Abstract

Polycrystalline Er-Sc silicates ($Er_xSc_{2-x}Si_2O_7$ and $Er_xSc_{2-x}SiO_5$) were fabricated using multilayer nanostructured films of $Er_2O_3/SiO_2/Sc_2O_3$ deposited on SiO_2/Si substrates by RF sputtering and thermal annealing at high temperature. The films were characterized by synchrotron radiation grazing incidence X-ray diffraction, cross-sectional transmission electron microscopy, energy-dispersive X-ray spectroscopy, and micro-photoluminescence measurements. The Er-Sc silicate phase $Er_xSc_{2-x}Si_2O_7$ is the dominant film, and Er and Sc are homogeneously distributed after thermal treatment because of the excess of oxygen from SiO_2 interlayers. The Er concentration of 6.7×10^{21} atoms/cm^3 was achieved due to the presence of Sc that dilutes the Er concentration and generates concentration quenching. During silicate formation, the erbium diffusion coefficient in the silicate phase is estimated to be 1×10^{-15} cm^2/s at 1,250°C. The dominant $Er_xSc_{2-x}Si_2O_7$ layer shows a room-temperature photoluminescence peak at 1,537 nm with the full width at half maximum (FWHM) of 1.6 nm. The peak emission shift compared to that of the Y-Er silicate (where Y and Er have almost the same ionic radii) and the narrow FWHM are due to the small ionic radii of Sc^{3+} which enhance the crystal field strength affecting the optical properties of Er^{3+} ions located at the well-defined lattice sites of the Sc silicate. The Er-Sc silicate with narrow FWHM opens a promising way to prepare photonic crystal light-emitting devices.

Keywords: Rare-earth doping; Photoluminescence; Thin films

Background

The realization of Si photonics requires a series of components, including continuous-wave (CW) coherent light sources, modulators, amplifiers, switches, detectors, and couplers. Great efforts have been made to fabricate these various components, and successes have been achieved to some degree: Modulators based on the electro-absorption effect [1-4] have been demonstrated, Si-based avalanche photodetectors with a 340-GHz gain bandwidth product have been realized [5], a nanophotonic switch has been made by IBM [6], and on-chip and off-chip couplers have also been demonstrated [7,8]. Among these components, coherent light sources and amplifiers are the most challenging because of the lack of a Si-compatible high-gain material. Bulk Si is a very inefficient emitter because of its indirect bandgap. An alternative approach is to introduce rare-earth ions as impurities into Si [9]. Erbium-doped materials are widely studied as active media in planar Si-compatible optical amplifiers [10,11] owing to the radiative emission of erbium at 1.54 μm, which is a strategic wavelength for telecommunications [12-14].

However, obtaining room-temperature erbium luminescence from doped silicon is not easy, mainly because of the low solubility of erbium in bulk silicon, small emission cross section, and very strong non-radiative coupling between erbium ions and the silicon host. The time constant of the non-radiative transfer mechanisms is much shorter than that of the erbium luminescence (microseconds and milliseconds, respectively) [13,15]. A promising solution could be the use of rare-earth (RE) compounds, which permit us to gradually insert Er ions inside a proper crystalline structure, by substituting RE ions with Er ions, and thus avoid their clusterization [16]. Recently, Er silicates have been reported by many researchers as a possible alternative [17,18] to demonstrate optical amplification. Er, a major constituent instead of a dopant, can provide optically active Er concentrations that exceed 10^{22} cm^{-3} [19]. However, pure Er silicates are not suitable for 1.54-μm applications as the extremely

* Correspondence: Adel.Najar@lab.ntt.co.jp
[1]NTT Basic Research Laboratories, NTT Corporation, 3-1, Morinosato-Wakamiya, Atsugi, Kanagawa 243-0198, Japan
Full list of author information is available at the end of the article

high Er concentration leads to effects such as concentration quenching and cooperative up-conversion, which introduce strong non-radiative recombination paths for the 1.54 μm luminescence [19,20]. Lo Savio et al. have shown that Y-Er disilicate ($Y_{2-x}Er_xSi_2O_7$) is a good host candidate since it affords a maximum solubility of 10^{22} cm^{-3}, which is due to the same crystalline structure with very similar lattice parameters in the constituent materials ($Er_2Si_2O_7$ and $Y_2Si_2O_7$) and because both Er and Y atoms occupy the same atomic sites [21]. Scandium ions (Sc^{3+}), on the other hand, present a smaller size (ionic radius = 0.75 Å) compared to erbium (Er^{3+}) (ionic radius = 0.881 Å). Generally, this can result in enhancing crystal field strength for Er dopants, silicates, and oxides [16,22]. In fact, Fornasiero et al. synthesized single crystal of Er-doped Sc silicates using the Czochralski technique with the idea that Sc^{3+} ions can increase the Stark splitting of the thermally populated erbium ground state as well as of other electronic energy levels of the silicates and therefore reduce reabsorption losses [16]. However, thin film growth of Er-Sc silicates on silicon wafer has not been established, and thus, the optical properties of the silicate have not been sufficiently characterized yet, compared with those of Er-Y silicates.

In this work, we have synthesized a polycrystalline Er-Sc silicate compound ($Er_xSc_{2-x}Si_2O_7$) in which Er and Sc are homogeneously distributed using RF sputtering with multilayer Er_2O_3, Sc_2O_3, and SiO_2 layers deposited on SiO_2/Si (100) substrate and thermal annealing at high temperature. The diffusion coefficient of Er was determined after annealing at 1,250°C. The photoluminescence of the dominant phases of the Er-Sc silicate was reported and discussed.

Methods

Er-Sc multilayer thin films were grown by RF sputtering by alternating 15-nm-thick layers of Er_2O_3 and Sc_2O_3 separated by a 15-nm-thick SiO_2 layer. These layers were deposited on 50-nm-thick Er_2O_3 on SiO_2 (1.3 μm)/Si (100) substrate at room temperature. After deposition, the samples were annealed in O_2 at 1,250°C for 1 h. The samples were analyzed by atomic force microscopy (AFM), using cross-sectional transmission electron microscopy (TEM)/energy-dispersive X-ray spectroscopy (EDS) images obtained at 200 keV, and by synchrotron radiation grazing incidence X-ray diffraction (GIXD) experiments that were performed on the as-grown and annealed samples at the BL24XU in SPring-8 (Hyogo, Japan) using an X-ray wavelength of 1.24 Å and an incidence angle of 1.0° [23]. Photoluminescence (PL) measurements were performed using a laser at 1,527.6 nm with an excitation power of 125 mW at 4 and 300 K. The excitation laser was focused to a spot with a diameter of about 15 μm and an incident angle of 45° through an objective lens. The luminescence from the sample was collected perpendicularly with a different objective lens with a numerical aperture of 0.40 [24]. The PL spectra were detected using a 0.5-m spectrometer and cooled InGaAs detector [23,25].

Results and discussion

GIXD profiles of the crystalline structure after the deposition and annealing of the films are shown in Figure 1. The inset image illustrates the multilayer structure before annealing. The GIXD profile of the sample after deposition shows the presence of Er_2O_3, $Er_2Si_2O_7$, and $Sc_2Si_2O_7$ in the films. After the annealing at 1,250°C, peaks with high intensity are assigned to $Er_2Si_2O_7$ and Er_2SiO_5 phases. After annealing, we have only $Er_2Si_2O_7$ and Er_2SiO_5 because of the diffusion of Er and Sc in different layers and the formation of new polycrystalline mixed compounds assigned to $Er_xSc_{2-x}Si_2O_7$ and $Er_xSc_{2-x}SiO_5$. Moreover, it has been demonstrated that in the Yb-Er disilicate or Y-Er disilicate, Er^{3+} can be substituted with Y^{3+}, Yb^{3+}, or Tm^{3+} ions because they have similar ionic radii, whereas Sc^{3+} ions have small radii that affect the crystalline structure of the Er-Sc silicate.

To determine the microscopic structures of the existing phases ($Er_xSc_{2-x}SiO_5$, $Er_xSc_{2-x}Si_2O_7$, Er_2O_3) after deposition, we performed TEM analysis of the cross section coupled to EDS measurements and selected area electron diffraction (SAED) images of the samples after deposition and annealing at 1,250°C. The cross-sectional image in Figure 2a obtained after deposition shows different layers of Er_2O_3, Sc_2O_3, and SiO_2 with a total deposition thickness of around 109 nm. In Figure 2a, the inset SAED image from the Er_2O_3 layer at the bottom shows multicrystalline rings. The interplanar spacings

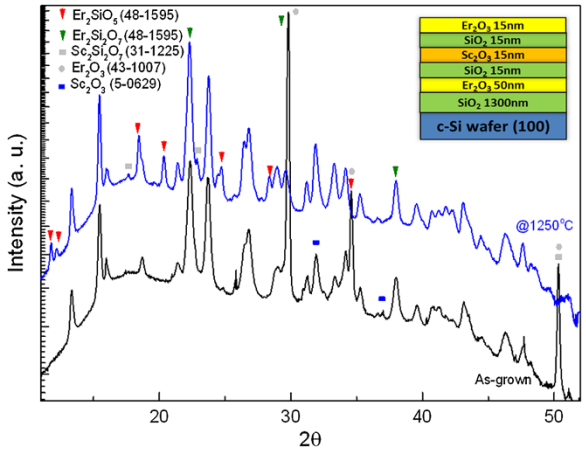

Figure 1 Synchrotron radiation GIXD obtained from the samples after deposition and annealing at 1,250°C for 1 h in O_2. The Joint Committee on Powder Diffraction Standards (JCPDS) numbers correspond to different compounds. The inset shows the fabricated structure.

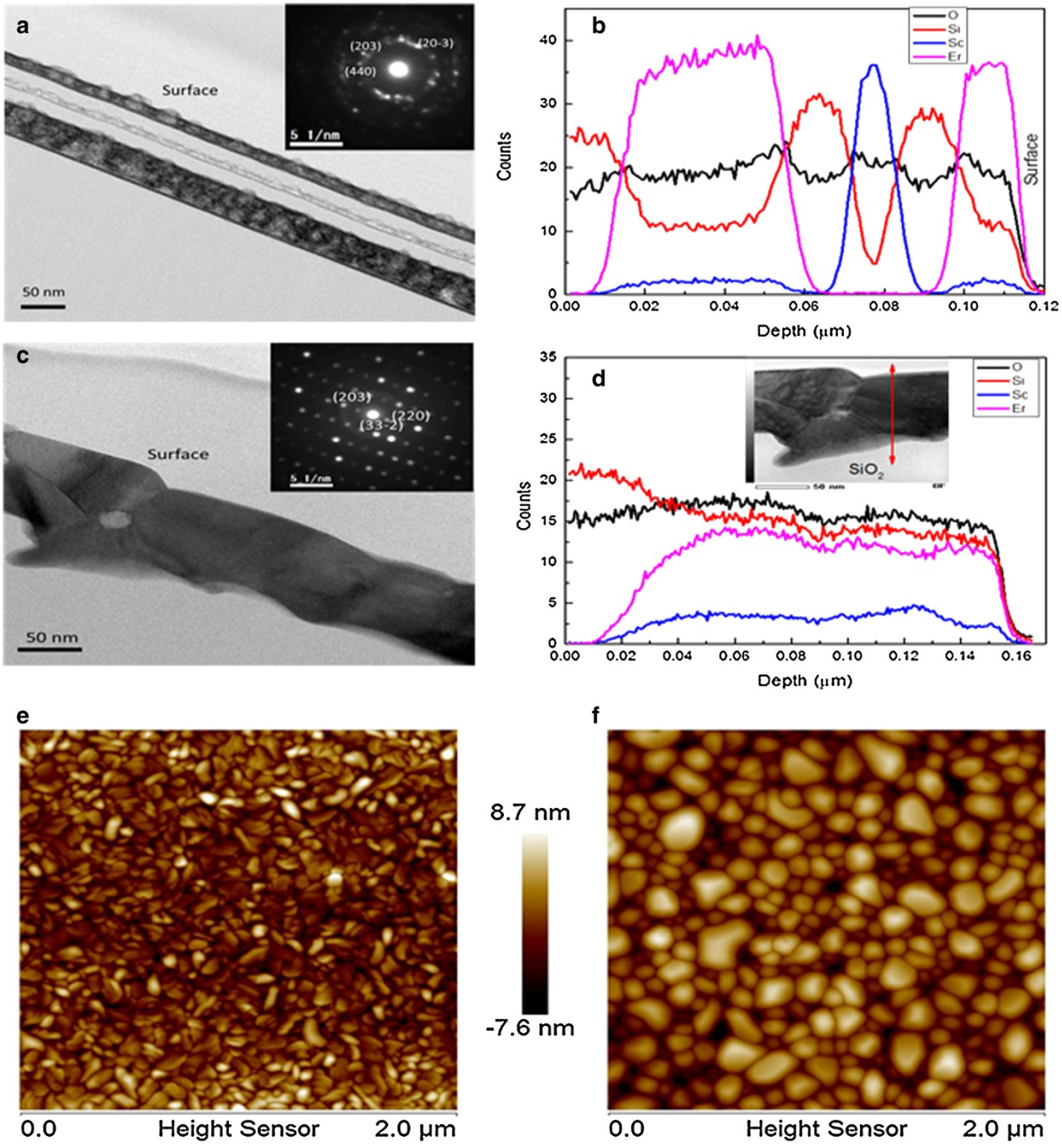

Figure 2 Cross-sectional TEM images, EDS concentration profiles, and AFM images. (a, c) Cross-sectional TEM images before and after annealing at 1,250°C with SAED images in the insets. **(b, d)** EDS concentration profiles of Er, Sc, O, and Si for the corresponding inset TEM images **(a)** and **(c)**, respectively. **(e, f)** AFM images of the sample after deposition and annealing at 1,250°C.

(*d*) are about 1.29, 1.32, and 1.52 Å, corresponding respectively to (203), (440), and (20-3) planes, for $Er_2Si_2O_7$ and 1.32 and 1.52 Å, corresponding respectively to (800) and (444) planes, for Er_2O_3. The same phases ($Er_2Si_2O_7$ and Er_2O_3) are identified in the top layer of Er_2O_3. The corresponding EDS profiles obtained from the samples after deposition are shown in Figure 2b with discontinuity of Er and Sc concentration profiles in the deposition layers.

After thermal treatment at 1,250°C in O_2, we formed a unique layer with an average thickness of 102 nm as shown in Figure 2c. The SAED images show a single-crystal compound. The interplanar spacings are 1.30, 1.54, and 2.61 Å, corresponding respectively to (203), (33-2),

and (220) planes, for $Er_2Si_2O_7$. The annealing treatment at 1,250°C results in the intermixing between different layers with homogeneous concentration profiles of Er, Sc, Si, and O in depth (Figure 2c). Indeed, Er and Sc diffuse in the SiO_2 layer. EDS measurements show that Er and Sc concentrations are 6.7×10^{21} and 1.4×10^{21} atoms/cm^3, respectively, with the Er/Sc ratio of 4.5. This high concentration of Er incorporated into the Sc_2O_3 matrix is due to the presence of Sc that creates concentration quenching. From the GIXD and TEM analysis, we conclude that $Er_2Si_2O_7$ is in the bottom and top layers before annealing and that the $Er_xSc_{2-x}Si_2O_7$ phase is dominant after annealing at 1,250°C. In addition, it is considered that the high-temperature annealing at 1,250°C and long annealing time enhance the reaction of Er-O and Si-O precursors with the SiO_2 interlayers, converting most of the Er_2SiO_5 to $Er_2Si_2O_7$ [18]. The existence of the $Er_xSc_{2-x}SiO_5$ phase after annealing determined by GIXD analysis may be due to size of the analyzed surface which is much bigger using an X-ray beam than a TEM electron beam. The surface morphology after deposition and annealing was analyzed by AFM. The AFM images in Figure 2e,f show a flat surface with no cracks after annealing up to 1,250°C. After deposition, the roughness value of approximately 2.7 nm was measured against that of 4.1 nm after annealing because of the increase of the grain size.

Er diffusion at 1,250°C was analyzed by measuring the Er concentration profiles before and after heat treatment in Figure 3. After deposition, the atomic weight of Er is estimated to be 35% to 40%, and these values decrease from 11% to 14% after annealing at 1,250°C due to the homogeneous redistribution of Er atoms in the annealing layers. Er diffuses in the depth with a diffusion length of around 39 nm in the bottom layer of SiO_2 compared to the as-grown sample (Figure 3), but we suppose that Er diffuses with the same thickness in the other layers. The diffusion length is given by $L = 2\sqrt{Dt}$, where D is the diffusion coefficient and t is the duration of the thermal treatment. For the annealing temperature of 1,250°C, the diffusion coefficient D is 1×10^{-15} cm^2/s. This value is fairly consistent with the value of 0.63×10^{-15} cm^2/s for Er in the SiO_2 layer prepared by magnetron sputtering and annealed at 1,100°C for 1.5 h in N_2 [26] and about 2 orders of magnitude higher than the diffusion coefficient of silicon-rich silicon oxide (SRSO) of 1.2×10^{-17} cm^2/s at 1,100°C [27].

The PL in the range from 1,533 to 1,555 nm was measured in the sample annealed at 1,250°C, at 4 K, and at room temperature using 1,527.6-nm excitation wavelength, which corresponds to the energy between the ground state ($^4I_{15/2}$) and second higher excited state ($^4I_{13/2}$), with 125-mW excitation power. As shown in Figure 4, PL spectra exhibit the same shape for both temperatures with the main emission peak at 1,537 with sub-peaks at 1,546.2 and 1,551 nm corresponding to the energy levels of Er^{3+} ions. The peak at 1,537 nm corresponds to the energy between Er^{3+} ($^4I_{15/2}$) and Er^{3+} ($^4I_{13/2}$) ions in the Sc silicate phase with the full width at half maximum (FWHM) of 1.6 nm at room temperature and 4 K. We attribute this enhancement to the narrow emission peak of $Er_xSc_{2-x}Si_2O_7$ to the well-defined lattice sites for Er^{3+}. This narrow emission will be very promising for photonic crystal light-emitting devices because the extraction efficiency can be increased with a pronounced narrowing of the emission. Shin and Lee have shown a peak emission at 1,529 nm with an FWHM of 11 nm for $Er_xY_{2-x}SiO_5$ annealed at 1,200°C using an excitation wavelength of 488 nm [28]. In addition, Miritello et al. obtained a peak emission at 1,535 nm for

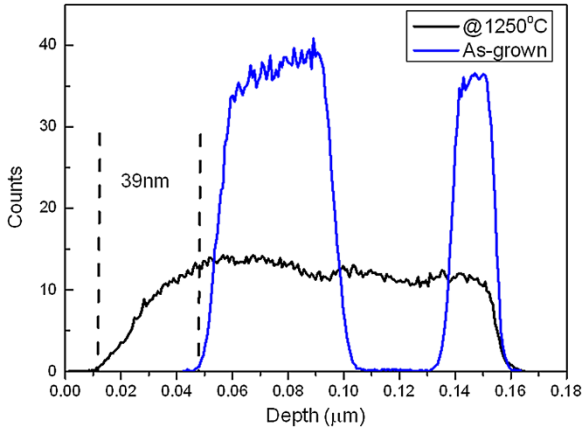

Figure 3 EDS concentration profiles of Er after deposition and annealing at 1,250°C.

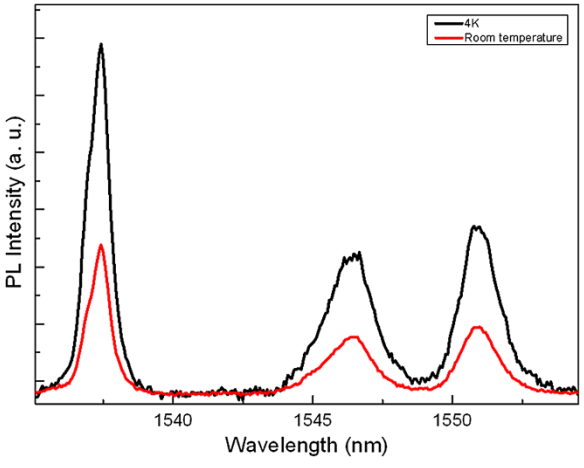

Figure 4 PL spectra at room temperature and 4 K obtained from the sample annealed at 1,250°C.

α-$(Yb_{1-x}Er_x)_2Si_2O_7$ with a 37-nm FWHM using 532 nm excitation wavelength after annealing at 1,200°C [29]. The GIXD and SAED results confirm the emission peaks corresponding to the dominant $Er_xSc_{2-x}Si_2O_7$ phase. Furthermore, the peak energies are different from the Stark level splitting of Er energy levels in Er-doped $Sc_2Si_2O_7$ and Sc_2SiO_5 single crystals at low temperature identified by Fornasiero et al. [16] and Omi et al. [30]. Since both Sc and Y are optically inactive in the matrix, in this way, it is possible to control the Er pair interactions and maximize the Er active concentration. The advantage of using Sc in comparison to Y is that the radius of Sc is smaller compared to those of Y and Er. This smaller radius enhances the crystal field strength which affects the luminescence properties with smaller FWHM compared to the effect of Y. However, Er can be substituted with Y in the silicate phase which is not the case for Sc due to the radius effect.

The crystal field strength parameters are defined by [31] $N_V = \left[\sum_{k,q} \frac{4\pi}{2K+1}\left(B_q^k\right)^2\right]^{1/2}$, where B_q^k is the crystal field parameters that affect the Stark levels of Er^{3+}, which characterize the interaction between ligands and the central ions and include the radial integral of the wavefunction. The values of the crystal field strength parameters N_V have been calculated for Er^{3+} doped in different matrices: Sc_2O_3 (5,300 cm^{-1}), Y_2O_3 (2,700 cm^{-1}), and Er_2O_3 (2,200 cm^{-1}) [32,33], and show clearly that the crystal field strength increases regularly with decreasing ionic radius of the RE host cation, which generates the Stark splitting energy levels. In our case, the 8-nm redshift is due to the presence of Sc ions, which increase the crystal field strength and thereby enhance the Stark splitting of the thermally populated Er energy levels ($^4I_{15/2}$ and $^4I_{13/2}$ levels) as well as that of the other electronic energy levels.

Conclusions

In summary, a polycrystalline $Er_xSc_{2-x}Si_2O_7$-dominant compound was fabricated using RF sputtering by alternating Er_2O_3 and Sc_2O_3 layers separated by a SiO_2 layer and annealed in O_2 gas. After high-temperature annealing at 1,250°C, the Er and Sc ions are distributed homogeneously in the layer. The erbium diffusion coefficient in the SiO_2 at the annealing temperature was estimated to be 1×10^{-15} cm^2/s. The Er-Sc silicate layer shows a sharp emission peak at room temperature centered at 1,537 nm as a result of the strong crystal field strength generated by the small ionic radii of Sc^{3+} ions. The Er-Sc silicate could be used as an efficient material for photonic devices.

Competing interests

The authors declare that they have no competing interests.

Authors' contributions

AN designed and fabricated the structure and carried out the experiments as well as the analyses. HO carried out the GIXD experiments and the analysis of data. TT carried out the PL measurements and the analysis of data. All authors read and approved the final manuscript.

Acknowledgements

We thank Dr. Shingo Takeda for his help in the synchrotron radiation experiments at beam line BL24XU in SPring-8. This work was partially supported by JSPS KAKENHI Grant Number 24360033.

Author details

[1]NTT Basic Research Laboratories, NTT Corporation, 3-1, Morinosato-Wakamiya, Atsugi, Kanagawa 243-0198, Japan. [2]NTT Nanophotonics Center, NTT Corporation, 3-1, Morinosato-Wakamiya, Atsugi, Kanagawa 243-0198, Japan.

Received: 18 June 2014 Accepted: 6 July 2014
Published: 15 July 2014

References

1. Liu J, Beals M, Pomerene A, Bernardis S, Sun R, Cheng J, Kimerling LC, Michel J: **Waveguide-integrated, ultralow-energy GeSi electro-absorption modulators.** *Nat Photon* 2008, **2:**433.
2. Emboras A, Briggs RM, Najar A, Nambiar S, Delacour C, Grosse P, Augendre E, Fedeli JM, Salvo B, Atwater HA, Espiau de Lamaestre R: **Efficient coupler between silicon photonic and metal-insulator-silicon-metal plasmonic waveguides.** *Appl Physics Lett* 2012, **101**(25):251117.
3. Emboras A, Najar A, Nambiar S, Grosse P, Augendre E, Leroux C, Salvo B, Espiau de Lamaestre R: **MNOS stack for reliable, low optical loss, Cu based CMOS plasmonic devices.** *Opt Express* 2012, **20**(13):13612.
4. Xu Q, Schmidt B, Pradhan S, Lipson M: **Micrometre-scale silicon electro-optic modulator.** *Nature* 2005, **435:**325.
5. Kang Y, Liu HD, Morse M, Paniccia MJ, Zadka M, Litski S, Sarid G, Pauchard A, Kuo YH, Chen HW, Sfar Zaoui W, Bowers JE, Beling A, McIntosh DC, Zheng X, Campbell JC: **Monolithic germanium/silicon avalanche photodiodes with 340 GHz gain-bandwidth product.** *Nat Photon* 2008, **3:**59.
6. Vlasov Y, Green WMJ, Xia F: **High-throughput silicon nanophotonic deflection switch for on-chip optical networks.** *Nat Photon* 2008, **2:**242.
7. McNab SJ, Moll N, Vlasov YA: **Ultra-low loss photonic integrated circuit with membrane-type photonic crystal waveguides.** *Opt Express* 2003, **11:**2927.
8. Analui B, Guckenberger D, Kucharski D, Narasimha A: **A fully integrated 20-Gb/s optoelectronic transceiver implemented in a standard 0.13-μm CMOS SOI technology.** *IEEE J Solid-State Circuits* 2006, **41:**2945.
9. Kenyon AJ: **Erbium in silicon.** *Semicond Sci Technol* 2005, **20:**R65.
10. Najar A, Charrier J, Ajlani H, Lorrain N, Haesaert S, Oueslati M, Haji L: **Optical gain at 1.53 μm in Er^{3+}–Yb^{3+} co-doped porous silicon waveguides.** *Mater Sci Eng B* 2007, **146**(1):260.
11. Lee J, Shin JH, Park N: **Optical gain at 1.5 μm in nanocrystal Si-sensitized Er-doped silica waveguide using top-pumping 470 nm LEDs.** *J Lightwave Technol* 2005, **23**(1):19.
12. Najar A, Ajlani H, Charrier J, Lorrain N, Haesaert S, Oueslati M, Haji L: **Optical study of erbium-doped-porous silicon based planar waveguides.** *Physica B* 2007, **396**(1):145.
13. Polman A: **Erbium implanted thin film photonic materials.** *J Appl Phys* 1997, **82**(1):1.
14. Najar A, Lorrain N, Ajlani H, Charrier J, Oueslati M, Haji L: **Er^{3+} doping conditions of planar porous silicon waveguides.** *Appl Surf Sci* 2009, **256**(3):581.
15. Palm J, Gan F, Zheng B, Michel J, Kimerling LC: **Electroluminescence of erbium-doped silicon.** *Phys Rev B* 1996, **54:**17603.
16. Fornasiero L, Petermann K, Heumann E, Huber G: **Spectroscopic properties and laser emission of Er^{3+} in scandium silicates near 1.5 μm.** *Opt Mater* 1998, **10:**9.
17. Suh K, Shin JH, Seo SJ, Bae BS: **Large-scale fabrication of single-phase Er_2SiO_5 nanocrystal aggregates using Si nanowires.** *Appl Phys Lett* 2006, **89**(22):223102.
18. Wang XJ, Nakajima T, Isshiki H, Kimura T: **Fabrication and characterization of Er silicates on SiO_2/Si substrates.** *Appl Phys Lett* 2009, **95**(4):041906.

19. Miritello M, Lo Savio R, Iacona F, Franzó G, Irrera A, Piro AM, Bongiorno C, Priolo F: **Efficient luminescence and energy transfer in erbium silicate thin films.** *Adv Mater* 2007, **19**(12):1582.
20. Suh K, Shin HJ, Seo SJ, Bae BS: **Er^{3+} luminescence and cooperative upconversion in $Er_xY_{2-x}SiO_5$ nanocrystal aggregates fabricated using Si nanowires.** *Appl Phys Lett* 2008, **92:**121910.
21. Lo Savio R, Miritello M, Shakoor A, Cardile P, Welna K, Andreani LC, Gerace D, Krauss TF, O'Faolain L, Priolo F, Galli M: **Enhanced 1.54 μm emission in Y-Er disilicate thin films on silicon photonic crystal cavities.** *Opt Express* 2013, **21**(8):10278.
22. Stanek CR, McClennan KJ, Uberuaga BP, Sickafus KE: **Determining the site preference of trivalent dopants in bixbyite sesquioxides by atomic-scale simulations.** *Phys Rev B* 2007, **75:**134101.
23. Michael CP, Yuen HB, Sabnis VA, Johnson TJ, Sewell R, Smith R, Jamora A, Clark A, Semans S, Stanckovic SPB, Painter O: **Growth, processing, and optical properties of epitaxial Er_2O_3 on silicon.** *Opt Express* 2008, **16:**19649.
24. Tawara T, Omi H, Hozumi T, Kaji R, Adachi S, Gotoh H, Sogawa T: **Population dynamics in epitaxial Er_2O_3 thin films grown on Si (111).** *Appl Phys Lett* 2013, **102:**241918.
25. Omi H, Tawara T: **Energy transfers between Er^{3+} ions located at the two crystalographic sites of Er_2O_3 grown on Si(111).** *Jap J Appl Phys* 2012, **51:**02BG07.
26. Lu YW, Julsgaard B, Christian Petersen M, Skougaard Jensen RV, Garm Pedersen T, Pedersen K, Larsen NA: **Erbium diffusion in silicon dioxide.** *Appl Phys Lett* 2010, **97:**141903.
27. Talbot E, Larde R, Pareige P, Khomenkova L, Hijazi K, Gourbilleau F: **Nanoscale evidence of erbium clustering in Er-doped silicon-rich silica.** *Nanoscale Res Lett* 2013, **8:**39.
28. Shin JH, Lee M: **Reducing optical losses and energy-transfer upconversion in $Er_xY_{2-x}SiO_5$ waveguides.** *IEEE Photonics Technol Letters* 1801, **2013:**25.
29. Miritello M, Cardile P, Lo Savio R, Priolo F: **Energy transfer and enhanced 1.54 μm emission in erbium-ytterbium disilicate thin films.** *Optics Express* 2011, **19**(21):20761.
30. Omi H, Tawara T, Tateishi M: **Real-time synchrotoron radiation X-ray diffraction and abnormal temperature dependence of photoluminescence from erbium silicates on SiO_2/Si substrates.** *AIP Adv* 2012, **2**(1):012141.
31. Auzel F, Malta O: **A scalar crystal field strength parameter for rare-earth ions: meaning and usefulness.** *J Phys* 1983, **44:**201.
32. Antic-Fidancev E, Holsa J, Lastusaari M: **Crystal field strength in C-type cubic rare earth oxides.** *J Alloys Compd* 2002, **341:**82–86.
33. Trabelsi I, Maâlej R, Dammak M, Lupei A, Kamoun M: **Crystal field analysis of Er^{3+} in Sc_2O_3 transparent ceramics.** *J Lumin* 2010, **130:**927–931.

doi:10.1186/1556-276X-9-356
Cite this article as: Najar *et al.*: Scandium effect on the luminescence of Er-Sc silicates prepared from multi-nanolayer films. *Nanoscale Research Letters* 2014 **9**:356.